



POLARIZING VIEWS

By Stephen Guimond, Meadowlark Optics Inc.,
and David Elmore, High Altitude Observatory,
National Center for Atmospheric Research

Designing effective crystal waveplates requires understanding the engineering tradeoffs.

Precision control of polarization is increasingly important in disciplines such as solar polarimetry, optical communications, biomedical imaging, military target identification, chemical analysis, and wavelength filtering. Designers generally choose waveplates, or phase retarders, to alter or analyze the state of polarization, but often overlook their performance over the wavelength bandwidth, operating temperature, or field of view (FOV). With a command of the tradeoffs, the engineer can specify a polarization optic with reduced sensitivity to angle of incidence, temperature change, or wavelength.

Achromatic waveplates commonly take one of three forms: devices exploiting total internal reflection, such as

Fresnel rhombs; single-material devices exploiting a series of fast-axis orientations to achieve achromaticity, such as Pancharatnam devices; and multi-material devices that balance the birefringence dispersion of the materials to achieve achromatic performance, such as the common quartz-magnesium fluoride waveplate.^{1,2}

Rhombs are highly achromatic but bulky, and often present an output beam displaced from the input beam. Polymer Pancharatnam devices are less expensive than crystal optics but have a wavelength-dependent fast axis orientation. The bi-crystalline achromatic waveplate is a dependable workhorse device and we'll use its simple design to demonstrate design strategies and performance tradeoffs.

POLARIZATION 101

Light is an electromagnetic wave of frequency ν and wavelength λ . All light in our discussion is monochromatic and completely polarized. The polarization direction is the same as that of the electric field vector. We represent the electromagnetic wave propagating along the z-axis as the sum of two co-propagating, orthogonal waves: one whose electric field oscillates along the x-axis, the other along the y-axis (see figure 1). The relative phase between these two waves (in radians) is ϕ so the spatial displacement is $\phi\lambda/2\pi$.

The resultant electric field is the vector sum of these two components. The resultant vector varies in time as the wave passes through the x-y plane. The tip of that vector sweeps out shapes in time dictated by the difference in phase between its x- and y-components. We observe these shapes from the z-axis, looking toward the source. These shapes define the polarization state as linear (phase delay $\phi=0$), circular ($\phi=\pi/2$), or elliptical ($\phi=0.35 \cdot 2\pi$, for example).

Birefringent materials can introduce phase delay. Birefringent materials demonstrate polarization-dependent indices of refraction; in other words, the x- and y-components of the electric field vector “experience” different indices of refraction as they travel through the birefringent medium, and consequently travel through the medium at different speeds. We call these indices the ordinary (n_o) and extraordinary (n_e) refractive indices. In figure 1, the x-component leads the y-component because the x-component is parallel to the fast axis (low index) and the y-component is parallel to the slow axis (high index).

We quantify the birefringence β as the difference in these indices: $\beta = \Delta n = n_e - n_o$.³ The difference in optical path length is proportional to the difference in indices of refraction. We express the path length difference, or retardance R , as $R = \beta t$, where t is the thickness of a medium of birefringence β . In units of waves, or fractions of 2π phase, we can express that retardance as $R_{\text{waves}} = \beta t / \lambda$. The phase delays of two layers of material, for example, add algebraically if the fast axis of one material is parallel (additive) or perpendicular (subtractive) to the fast axis of the other:

$$R_{\text{waves}}(\lambda) = \frac{1}{\lambda} [\beta_1 t_1 + \beta_2 t_2] \quad [1]$$

DUALING WAVEPLATES

The design now rests simply in finding the crystal thicknesses t_1 and t_2 under design constraints such as achromatic operation, broad FOV, or athermal operation. For dual-wavelength or achromatic devices, we exploit the dependence of birefringence on wavelength. Birefringence, like refractive index, shows chromatic dispersion—that is, variation with wavelength. We characterize birefringence dispersion experimentally by fitting empirical models to

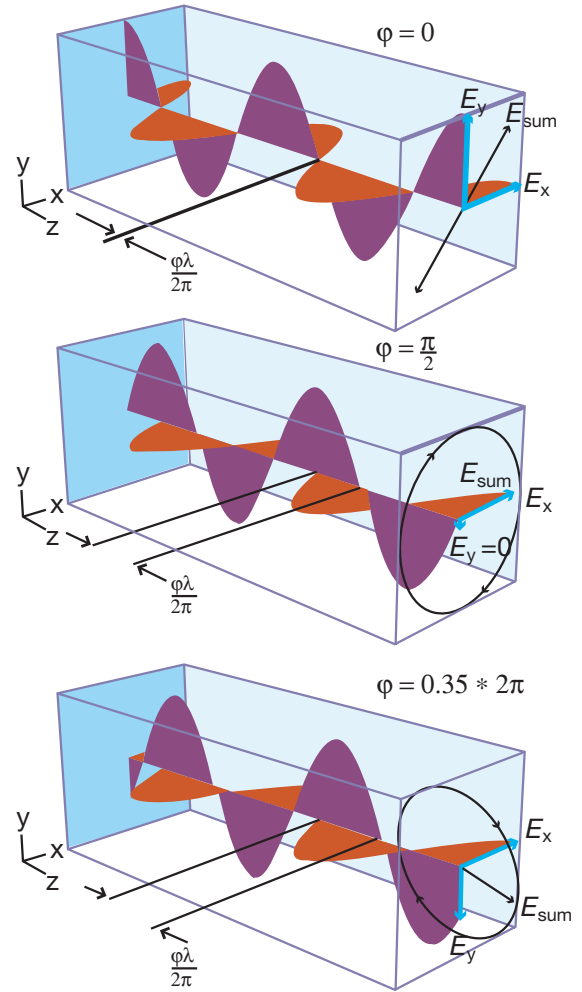


FIGURE 1 Polarized light can be represented as the sum of two orthogonal linear states. A phase delay $\phi=0$ between x- and y-components yields a resultant \mathbf{E}_{sum} that oscillates about a line oriented at 45° (linear polarization, top). If $\phi=\pi/2$, \mathbf{E}_{sum} maintains constant magnitude but rotates about the origin (circular polarization, middle). An arbitrary phase delay (for example, $\phi=0.35 \cdot 2\pi$) yields an \mathbf{E}_{sum} with varying magnitude and position (elliptical polarization, bottom).

spectropolarimetric measurements of various materials.⁴

A dual-wavelength waveplate must meet retardance specifications at two different wavelengths (λ_1 and λ_2). We express these constraints as

$$R_{\text{waves}}(\lambda_1) = \frac{1}{\lambda_1} [\beta_1(\lambda_1)t_1 + \beta_2(\lambda_1)t_2], \quad R_{\text{waves}}(\lambda_2) = \frac{1}{\lambda_2} [\beta_1(\lambda_2)t_1 + \beta_2(\lambda_2)t_2] \quad [2]$$

The two wavelengths λ_1 and λ_2 , and the retardances at these wavelengths $R_{\text{waves}}(\lambda_1)$ and $R_{\text{waves}}(\lambda_2)$, are specified by design. The birefringence dispersion curves of these

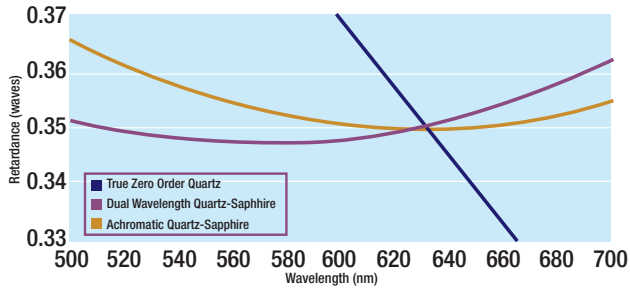


FIGURE 2 A comparison of retardance versus wavelength for a dual-wavelength waveplate (magenta) and an achromatic waveplate (yellow) shows that the slope is zero at the design wavelength (630 nm) for the achromat but not for the dual-wavelength part. The dual-wavelength part is 0.35λ at both 517 and 630 nm. A true zero order waveplate designed for 630 nm is also presented (blue).

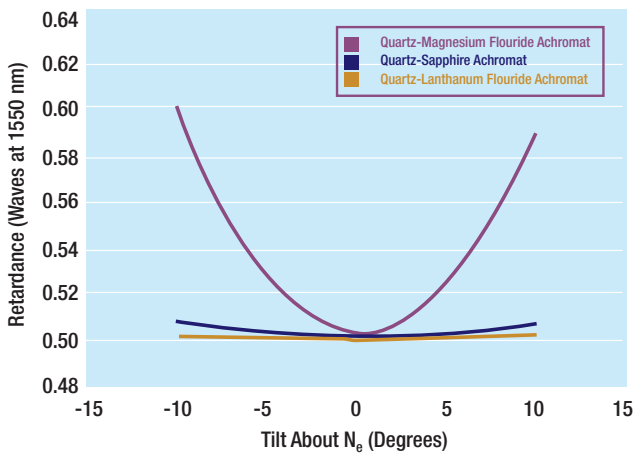


FIGURE 3 Plot of retardance versus incident angle for test data from three types of achromats shows a rapid change in retardance for the quartz-magnesium fluoride achromat (red) due to its constituents both having positive birefringence. Quartz-sapphire (blue) and quartz-lanthanum fluoride (yellow) achromats provide better performance.

materials $\beta_1(\lambda)$ and $\beta_2(\lambda)$ are given by nature. We need only calculate the thicknesses t_1 and t_2 to complete the design. Thickness is not an entirely free parameter, though; overly thin components suffer from poor flatness or transmitted wavefront distortion.

A negative thickness obtained from this calculation indicates that the fast axes of the dual waveplates are perpendicular. This configuration is sometimes called subtraction mode; addition mode refers to compound optics with parallel fast axes.

With the design complete, we polish the crystals to thickness, and mount or laminate the crystals for a compound optic that meets retardance specifications at both wavelengths.

ACHROMATIC DESIGN

We design achromatic waveplates similarly, but with a different constraint. Waveplates are achromatic when their retardance does not change over some wavelength range (see figure 2). In other words, the derivative of the retardance with respect to wavelength is zero at the design wavelength λ_0 .

$$\left. \frac{\partial R_{\text{waveplate}}(\lambda)}{\partial \lambda} \right|_{\lambda=\lambda_0} = 0 = \frac{1}{\lambda_0} \left[t_1 \frac{\partial \beta_1(\lambda_0)}{\partial \lambda} + t_2 \frac{\partial \beta_2(\lambda_0)}{\partial \lambda} \right] - \frac{1}{\lambda_0^2} [t_1 \beta_1(\lambda_0) + t_2 \beta_2(\lambda_0)] \quad [3]$$

To design the achromat we find the crystal thicknesses from the system of equations consisting of equation 1 and equation 3 evaluated at $\lambda=\lambda_0$.

Achromatic designs often pair quartz and magnesium fluoride because of their availability and optical quality. However, both quartz and magnesium fluoride have positive birefringence, which yields a waveplate with a poor FOV.⁵

Changes in incident angle affect the projection of the polarization state upon the index ellipsoid of the crystal and increase the path through the crystal. The resultant retardance increases or decreases depending upon whether the optic is tilted about the slow or fast axis, respectively. This characteristic allows us to precisely “tune” a waveplate, but can spell disaster for designs with uncollimated beams or alignment sensitivity.

Angular dependence goes as the sum of the two crystal thicknesses for pairs of like crystals (positive-positive or negative-negative) but is more forgiving for pairs of unlike sign. As negative crystals, sapphire or lanthanum fluoride yield excellent FOV when paired with quartz (see figure 3).

TEMPERATURE BALANCING

Retardance not only changes with wavelength, it also changes with temperature. Both crystal thickness and birefringence are temperature-dependent. By knowing material thermal properties, the designer can easily specify athermal waveplates.

We characterize materials by directly measuring their retardance under temperature control. We define the temperature coefficient as $\gamma = 1/R \cdot dR/dT$, where T is the temperature, and R the retardance in any units. This normalized temperature derivative represents the factor by which retardance changes per unit temperature change. To athermalize a waveplate composed of two different materials, we add the following constraint: $\gamma_1 R_1 + \gamma_2 R_2 = 0$, where again the subscripts denote the two materials. This assures that the change in retardance for material #1 is offset by that for material #2. Note that the sign between the terms would be negative for pairs of materials in subtraction mode.

To create an athermal design, we write the retardance and athermal constraints in terms of the crystal thicknesses:

$$R_{waves}(\lambda_0) = \frac{1}{\lambda_0} [\beta_1(\lambda_0)t_1 + \beta_2(\lambda_0)t_2] \quad [4]$$

$$\gamma_1\beta_1(\lambda_0)t_1 + \gamma_2\beta_2(\lambda_0)t_2 = 0 \quad [5]$$

Determining t_1 and t_2 , we have a part whose retardance is specified at a center wavelength, and whose retardance is stable over temperature changes (see figure 4). Note that it is not strictly possible to design the part to be achromatic *and* athermal. Two thicknesses—that is, two degrees of freedom—can not accommodate the three constraints of retardance, retardance slope, and temperature insensitivity; however, a little give and take with the specifications can lead to acceptable performance in all three.

LOOKING AT THE SUN

We put these principles to work when we designed and built a waveplate for a spectropolarimeter and polarimetric filtergraph being built by Lockheed Martin Solar and Astrophysics Laboratory (Palo Alto, CA) under contract to NASA. The instruments will be installed behind the 50-cm diameter optical telescope on Solar-B, a satellite to be launched August 2006 by the Institute for Space and Astronautical Science (Tokyo, Japan).

The waveplate is the polarization modulator for the instrument (see figure 4, bottom). To assure unchanged performance over a decade-long mission, we chose crystal over polymer. The mission required $0.35\lambda \pm 0.01$ of retardance at 630 nm and $0.35\lambda \pm 0.05$ at 517 nm; multi-order retardance was acceptable ($N \pm 0.35\lambda$). We had to maintain 0.0019λ stability over a 1° FOV and temperature range of 20°C to 40°C .

Our first approach followed the well-worn path to quartz and magnesium fluoride in a dual-wavelength design for 0.35λ but the crystals were too thin for the acoustic and vibrational loads of launch. Thicker parts for better robustness would not meet the retardance variation tolerance over the 1° FOV.

Our final design—quartz and sapphire—exploited the positive-negative pairing for better FOV. We had to make tradeoffs between the two constraints of a dual-wavelength part (0.35λ at both 517 nm and 630 nm) and the third constraint of athermal performance. The thermal constraint required the quartz and sapphire parts have a thickness ratio of 1.17. Our compromise: approximately maintain that ratio, while searching for dual-wavelength designs meeting the $N \pm 0.35\lambda$ specification. We succeeded with 5.35λ at 630 nm and 6.65λ at 517 nm. This solution was very close to the athermal ratio with a theoretical temperature coefficient below our ability to measure it.

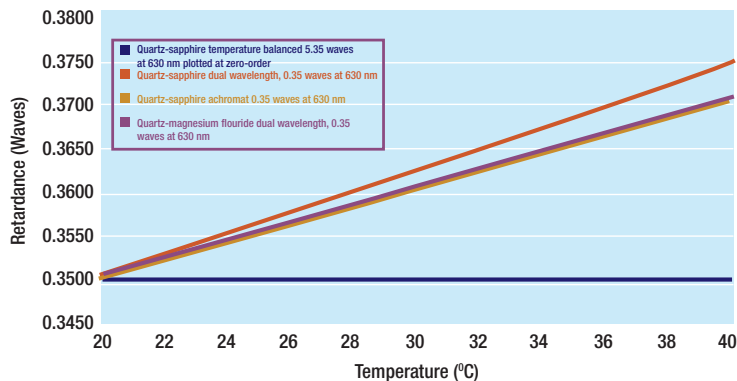
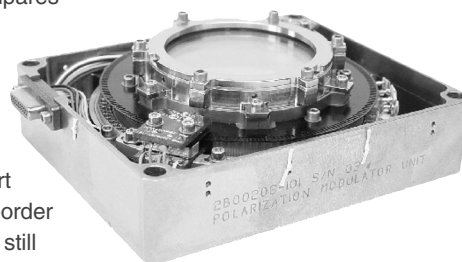


FIGURE 4 Plot (top) compares retardance versus temperature for a temperature-balanced part and several other designs. Note that the temperature-balanced part was designed to be multi-order (fifth order at 630 nm) yet still outperforms the zero-order compound parts presented with it. A polarization modulation unit (bottom), consisting of a rotation stage and the quartz-sapphire, temperature-balanced, dual-wavelength, high-FOV waveplate will be installed on the Solar-B satellite.



DAVID AKIN, LOCKHEED MARTIN

Empirical tests on the entire instrument from 10°C to 30°C measured an upper limit of 0.0016λ of variation for the waveplate, and the calculated variation over the 1° FOV was 0.0006λ so that both temperature variation and FOV met their 0.0019λ tolerances. The retarder also met the retardance tolerances at 630 nm and 517 nm—all demonstrating that successes in instrumentation are made one component design at a time. **oe**

Stephen Guimond is manufacturing engineering manager at Meadowlark Optics Inc., Frederick, CO; and David Elmore is lead engineer for the Solar-B spectro-polarimeter at the National Center for Atmospheric Research, operated by the University Corporation for Atmospheric Research under sponsorship of the National Science Foundation, Boulder, CO. For questions, contact Guimond at 303-833-4333, 303-833-4335 (fax), or sguimond@meadowlark.com.

References

1. S. Pancharatnam, *Indian Academy of Sciences Proceedings* 41, Sec. A, pg. 130 (1955).
2. J. Beckers, *Applied Optics* 10[4] p. 973 (1971).
3. E. Hecht and A. Zajac, *Optics*, Addison-Wesley Publishing Company, Reading, Massachusetts (1979).
4. K. Wildnauer, Agilent, personal communication.
5. P. Hale and G. Day, *Applied Optics* 27[24], p. 5146 (1988).

